



Whey protein isolate–chitosan interactions: A calorimetric and spectroscopy study

Hiléia K.S. de Souza^a, Guangyue Bai^b, Maria do Pilar Gonçalves^a, Margarida Bastos^{b,*}

^a REQUIMTE, Chemical Engineering Department, Faculty of Engineering, University of Porto, Rua Dr. Roberto Frias, 4200-465 Porto, Portugal

^b Centro de Investigação em Química (UP) – CIQ(UP), Department of Chemistry, Faculty of Sciences, University of Porto, Rua do Campo Alegre, 687, P-4169-007, Porto, Portugal

ARTICLE INFO

Article history:

Received 16 February 2009

Received in revised form 2 June 2009

Accepted 8 June 2009

Available online 17 June 2009

Keywords:

Whey proteins isolate

Chitosan

ITC

DSC

UV–vis spectrophotometry

ABSTRACT

Isothermal titration calorimetry (ITC) measurements were performed using solutions of whey protein isolate (WPI) and chitosan with different deacetylation degrees (DD), in acetate buffer solutions, pH 3–6. Turbidity measurements were performed in parallel in order to follow the changes in aggregation, so as to get deeper insight on the interaction mechanism. The viscosity–average molar mass of chitosan was obtained from intrinsic viscosity measurements, and the interaction enthalpies were derived at the studied pH values. Further, the denaturation process of α -lactalbumin and β -lactoglobulin within WPI was characterized by differential scanning calorimetry (DSC). At pH 3, where both chitosan and the proteins are positively charged, a weak carbohydrate–protein interaction is observed. When the pH is raised to 6, where the protein charge is expected to be negative, a much stronger interaction takes place. The results are discussed with special emphasis on the effect of pH on the interactions observed in this complex system.

© 2009 Elsevier B.V. All rights reserved.

1. Introduction

Whey proteins are milk proteins, which in their original media are dispersed in a continuous phase containing various salts ions and lactose. When used in food systems, whey proteins are usually denatured due to sample thermal treatments. As a result whey proteins aggregate, either in self-aggregation or with other food particles (e.g. casein micelles or emulsion droplets) [1,2]. In particular, they can interact with polysaccharide to form either soluble or insoluble complexes, depending on the colloidal properties of the protein/polysaccharide systems. These properties are related, not only to the individual functionality of protein and polysaccharide, but also to the nature and strength of the interactions between them. It is therefore very important to understand the effect of various factors, such as pH, ionic strength, concentration of whey protein isolate (WPI) and chitosan on the interactions.

Chitosan [(1-4)-2-amino-2-deoxy- β -D-glucan] is a linear polysaccharide (obtained by partial deacetylation of chitin after treatment with strong alkali at high temperature) with widespread applications in food processing, as well as in agriculture, biomedicine and as a micro-encapsulating agent [3]. The term chitosan embraces a series of polymers which vary in molar mass (M_w) and degree of deacetylation (DD). It is well known

that chitosan properties and interactions are dependent upon their molar mass and DD, which together with pH determine its global charge [3,4]. It is also known that it can adopt different space arrangements depending on the media, as e.g. a random coil in urea [5] or compact spheres in aqueous acetic acid [6]. Most chitosans have the ability to interact with anionic species. Recent results have shown that it seems particularly effective in reducing cholesterol blood levels in animals and in humans. This capacity has been explained on the basis of its positive charge which justifies the capacity to strongly bind negatively charged bile acids thorough electrostatic interactions [6]. The establishment of these interactions leads to the formation of anionic species/chitosan aggregation complexes [7–9], or “coacervates” when the anionic species is a lipid or a protein. These aggregates are used in many applications such as: fat substitution, protein separation, micro-encapsulation of drugs and additives, etc. In addition to its linear polymeric nature, its positive charge in acidic solutions turns it susceptible to be used as a polyelectrolyte. Indeed electrostatic protein–chitosan interaction depends significantly on pH. In aqueous solutions, chitosan becomes positively charged at $\text{pH} \leq 6.5$ due to the protonation of the amino groups $-\text{NH}_3^+$. When the pH is decreased, the intermolecular and intramolecular electrostatic repulsion between charged amino groups is increased and its solubility facilitated [10,11].

Isothermal titration calorimetry (ITC) is widely used to characterize the energetics of interactions [12]. Numerous studies have been reported in the literature that used ITC for the characterization of systems as different as β -lactoglobulin–sodium alginate

* Corresponding author. Tel.: +351 220402511; fax: +351 220402659.
E-mail addresses: hsouza@fe.up.pt (H.K.S. de Souza), gwbai@fc.up.pt (G. Bai), pilarg@fe.up.pt (M.d.P. Gonçalves), mbastos@fc.up (M. Bastos).

[13], polymer–solid [14], surfactant–polymer [15], protein–ligand interactions [16], enzyme receptor–ligand binding, etc. Viscosity measurements were performed in order to obtain the chitosan viscosity average molar mass (M_v) to enable a correct assignment of molar enthalpies [17].

The aim of this work was to study and characterize energetically the interaction between chitosan (with different DD) and WPI. Since pH influences the charge of both species, electrostatic complexes are expected to be formed in the pH window where WPI and chitosan have opposite charges. This should take place in the pH range of $5 < \text{pH} < 6$, as both species are positively charged for $\text{pH} < 5$ and chitosan is uncharged at $\text{pH} > 6$. Therefore the studies were performed in acetate buffer solutions at different pH values (3–6), by ITC and UV–vis spectrophotometry.

2. Experimental

2.1. Materials

A commercial whey protein isolate (WPI, LACTOPRODAN DI-9224) was obtained from Arla Foods Ingredients Ambh (Denmark) and used as the protein source. As specified by the manufacturer, the isolate contains a minimum of 93.5% total protein content, and the major protein constituents are: 74% β -lactoglobulin (β -LG, 18.36 kDa), 18% α -lactalbumin (α -LA, 14.5 kDa), 6% bovine serum albumin (BSA, 69 kDa). The isolate further contains lactose and fat (each at a maximum content of 0.2%), and minerals such as sodium (0.5%), potassium (1%), and calcium (0.1%). In order to quantify the enthalpy of denaturation on a molar basis to compare with literature values we did estimate an “average protein molar mass” as the percentage weighted average (according to manufacturer description) of the individual molar masses of each main component of the mixture. The obtained value was M_w 20.8 kDa.

Chitosan samples with two different degrees of deacetylation (Chit DD) Chit 90 and Chit 95 (with degrees of deacetylation of 90% and 95%, respectively) were obtained from Primex (Siglufjörður, Iceland). The approximate molar masses were supplied by the company: 150–200 kDa (Chit 95) and 250–300 kDa (Chit 90). The viscosity average molar masses were obtained from viscosity measurements.

Sodium acetate trihydrate ($\text{CH}_3\text{COONa}\cdot 3\text{H}_2\text{O}$) (Merck; 99.5%), glacial acetic acid (CH_3COOH) (Merck), and all other chemical were analytical grade and used without further purifications.

Purified water produced by a Milli-Q filtration system was used for the preparation of all solutions.

2.2. Solution preparation

The acetate buffer solutions were prepared by dissolving appropriate amounts of CH_3COOH and CH_3COONa in water so as to get the pH between 3 and 6, and always keeping the ionic strength equal to 0.100 mol L^{-1} . When necessary, the pH was adjusted to the desired value by the addition of aliquots of concentrated acetic acid.

The chitosan 0.7% (w/w) and WPI 0.5% (w/w) solutions were prepared by dissolving weighted amounts of the respective solid sample in the 0.100 mol L^{-1} acetate buffer. Both solutions were gently stirred for at least 2 h to ensure a complete dissolution and thereafter were stored at 278 K until approximately 1 h before the beginning of the experiment.

2.3. Methods

2.3.1. Determination of the chitosan viscosity–average molar mass

The intrinsic viscosity method can be used to determine the molar weight of chitosan.

Seven chitosan samples (concentration range from 0.015 to 0.006 g dL^{-1}) were prepared by dissolving chitosan in $\text{CH}_3\text{COOH}/\text{CH}_3\text{COONa}$ (AcOH/AcONa 0.250 mol L^{-1} aqueous solution at pH 4.7. These solutions had relative viscosities, η_{rel} , from about 2.0 to 1.2 to insure good accuracy and linearity of extrapolation to zero concentration. The viscosity of each sample was measured at $298.2 \pm 0.1 \text{ K}$, in a Cannon–Fenske glass capillary viscometer from Cometa (size 50, code: 5600051), using 7 mL of the solution. The flow time for the solvent (AcOH/AcONa 0.250 mol L^{-1} aqueous solution) was 204.12 s. All measurements were repeated three times for each sample and the uncertainty in flow time was determined to be 0.02 s.

The intrinsic viscosities of chitosan samples ($[\eta]$) were obtained by extrapolation to zero concentration of the experimental η_{sp}/c vs c and $\ln(\eta_{\text{rel}})/c$ vs c plots.

The intrinsic viscosity, $[\eta]$, was calculated by use of Huggins and Kraemer equations:

$$\frac{\eta_{\text{sp}}}{c} = [\eta] + k' [\eta]^2 c \quad (1)$$

$$\ln \frac{\eta_{\text{rel}}}{c} = [\eta] - k'' [\eta]^2 c \quad (2)$$

where c is the solution concentration in g dL^{-1} , η_{sp} is the specific viscosity ($\eta_{\text{sp}} = \eta_{\text{rel}} - 1$) and k' and k'' are dimensional constants that can be obtained from the Huggins and Kraemer plots for each polymer.

The viscosity–average molar mass, was finally estimated from the Mark–Houwink equation [17]:

$$[\eta] = KM_v^a \quad (3)$$

where K and a are constants for a given solute–solvent system and were calculated according to Kassai [17].

2.3.2. Differential scanning calorimetry (DSC)

DSC experiments were performed in a MicroDSC III (Setaram). A scan rate (β) of 1 K min^{-1} was used, and the sample was scanned between 293 and 368 K. The measurements were performed in standard cell with nominal volume of 1 mL.

The cell was charged with about 0.8 mL of a 10% (w/w) WPI solution in 0.100 mol L^{-1} acetate buffer at pH 6 and was rigorously weighted (to $\pm 0.0005 \text{ g}$). The weight of the reference cell (charged with buffer) was adjusted to within $\pm 0.0005 \text{ g}$.

The calorimetric denaturation curve for the WPI was collected against acetate buffer, and buffer–buffer runs were performed to be used as blank experiments. The instrument software (SETSOFT, Setaram) was used to perform the blank correction and to obtain the calorimetric enthalpy (ΔH_{cal}) by integration of the corresponding peak areas. The final C_p vs T plots were obtained by dividing the corrected signal by the scanning rate.

The original curve was deconvoluted into its components so as to separate the denaturation profile for each protein of WPI.

2.3.3. Isothermal titration microcalorimetry

The microcalorimeter unit used in this work consisted of a twin heat conduction calorimeter with 3 mL titration cell (ThermoMetric AB, Järfälla, Sweden), a water bath and its controller, built at Lund University, Sweden, and a $7\frac{1}{2}$ digit HP nanovoltmeter connected to the calorimetric channel and to the computer. The calorimetric unit used in this work as well as the instrumental procedure have been described in detail in our previous work [18,19].

Briefly, the volume of WPI solution in the calorimetric vessel was 2.6 mL. The calorimetric titration experiments consisted of a series of consecutive additions of a concentrated chitosan solution into WPI solutions. Dilution effects were taken care of separately, by titrating the same chitosan solution into acetate buffer solution in the vessel. The titrating solution was automatically added

Table 1

The viscosity-average molar mass (M_v) of Chit 90 and Chit 95 and the intrinsic viscosity ($[\eta]$), a , and K obtained for two chitosans in acetate buffer 0.25 mol L^{-1} at pH 4.7.

Samples	a	$K \times 10^5 \text{ (dL g}^{-1}\text{)}$	$[\eta] \text{ (dL g}^{-1}\text{)}$	$M_v \text{ (kDa)}$
Chit 90	0.73	54.61	5.53	330
Chit 95	0.68	103.7	4.39	225

in aliquots of $8.31 \mu\text{L}$ from a modified gastight Hamilton syringe through a thin stainless steel capillary until the desired range of chitosan concentrations had been covered. A special Kel-F turbine, made at Lund University workshop (Sweden) was used throughout at 100 rpm, as we have shown previously that it promotes very good mixing [18]. The instrument was calibrated electrically, by means of an insertion heater [20]. The experiments were performed in “fast mode”, and the recorded curves dynamically corrected thereafter [21,22]. All experiments were performed at $308.15 \pm 0.01 \text{ K}$ and were repeated at least three times.

2.3.4. Turbidity measurements

The turbidity (or optical dispersion, OD) of chitosan/WPI solutions was measured using an AGILENT 8453 UV-visible spectrophotometer, at a wavelength of 400 nm in a quartz sample cell with light path 10 mm, inserted in a block thermostated at 308.15 K by means of a water bath. The measured values of turbidity were corrected with the buffer used as a blank, and were only recorded after the values became stable (about 2–3 min) after thorough mixing the contents of the cell. Each reported value is the average of 3 consecutive readings.

Two different approaches were used to measure the turbidity properties of chitosan/WPI mixed solutions: (i) in order to study the effect of the chitosan concentration on the interaction, we did experiments where we added step-wise aliquots of the concentrated Chit 90 or Chit 95 (0.14% (w/w)) solution to WPI solution (0.5% (w/w)) in the pH range of 3–6. (ii) In order to understand the effect of pH on the turbidity properties of chitosan–WPI solutions, we did titrate aliquots of glacial acetic acid to the chitosan–WPI solutions, containing a WPI concentration of 0.5% (w/w) and chitosan concentrations of 2.37×10^{-3} or $2.40 \times 10^{-2} \text{ g dL}^{-1}$. The initial pH of the mixture was set at 6, and the pH values decrease with the step-wise addition of glacial acetic acid.

3. Results and discussion

3.1. Intrinsic viscosity and molar mass

The value of the constants a and K were calculated considering the solution ionic strength (I) as 0.25 mol L^{-1} . The results, summarized in Table 1, clearly show that the intrinsic viscosity of chitosan decreases with increasing DD. This behaviour could be explained by considering that a chain expansion of the chitosan molecules takes place as a consequence of the increasing repulsion between charged neighbour amino groups ($-\text{NH}_3^+$).

The determined M_v values were used to calculate the molar ratios of chitosan to WPI ($n_{\text{Chit}}/n_{\text{WPI}}$) for the studied systems in the ITC and OD experiments.

3.2. Differential scanning calorimetry

DSC study of the WPI was performed both as a means of determining the quality of the samples (by comparing the obtained thermodynamic data for the denaturation with published values for the component proteins) and mainly to insure that the proteins were not denatured at the temperature to be used in ITC and OD experiments.

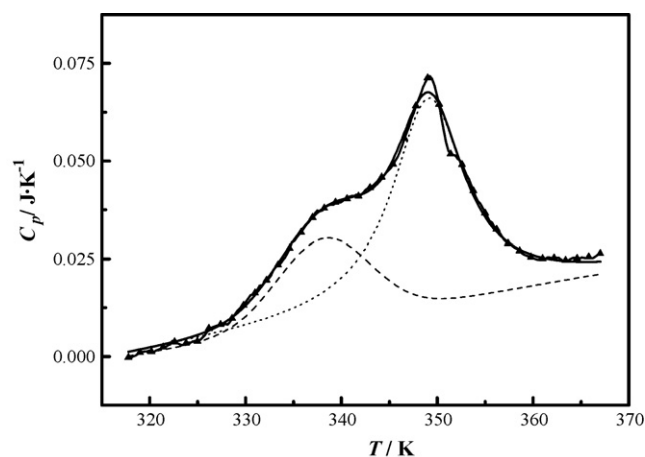


Fig. 1. Excess heat capacity as a function of temperature for WPI 10% (w/w) solutions (acetate buffer 0.100 mol L^{-1} (pH 6)). $\beta = 1 \text{ K min}^{-1}$. (—▲—) Original curve, (—) deconvoluted curve, (---) α -LA deconvoluted curve, (---) β -LG deconvoluted curve.

The calorimetric curves obtained by MicroDSC for the thermal denaturation process of WPI (10% (w/w)) in 0.100 mol L^{-1} acetate buffer (pH 6) are characterized by two endothermic processes that appear superimposed (Fig. 1). The shape of the obtained calorimetric curve is in good agreement with previously reported ones [23–25]. The original curve as well as the component ones obtained from deconvolution are shown in Fig. 1. We assign the two deconvoluted curves to the denaturation processes of α -LA and β -LG, as it has been reported that the two proteins denature independently [25]. The peak maxima for the C_p vs temperature curves was 338.19 K for α -LA and 348.97 K for β -LG, in agreement with the values reported in Ref. [24]. From the composition of the sample reported in Section 2.1 (α -LA 18% and β -LG 74%) and the total mass of sample in the calorimetric cell, we did calculate the mass of each protein in the sample. The respective calorimetric enthalpies (ΔH_{cal}) were obtained for α -LA and β -LG by independent integration of the deconvoluted curves, and the integral was normalized to the protein mass present in each case. The obtained enthalpies were: 1.686 and 0.847 J g^{-1} for α -LA and for β -LG respectively. The value for β -LG is in agreement with the one reported in Ref. [24], but the value for α -LA is significantly different. We should stress, however, that from their description it is not possible to ascertain how the calculation of the enthalpy was performed. The fact that it is in the first peak that we obtain a significant difference leads us to think that probably no deconvolution was attempted, and therefore the discrepancy is not surprising.

3.3. Thermodynamic description of the interaction process in chitosan/WPI systems

A typical microcalorimetric titration plot for the observed interaction between chitosan and WPI is presented in Fig. 2a, where the dilution curve of chitosan solution into acetate buffer is also included for comparison. It can be seen that for the chitosan/WPI system at pH 6 the global effect observed is exothermic, whereas the dilution of chitosan into acetate buffer at this pH value is an endothermic process. The corresponding values of the observed enthalpy changes (ΔH_{obs}) as a function of injection number are plotted in Fig. 2b for both processes. The enthalpies were calculated per mole of added chitosan.

Dilution experiments were taken care of separately, both for the dilution of chitosan and WPI. The dilution of WPI is not significant (results not shown) and therefore the results were only corrected for the chitosan dilution. The equations representing the processes

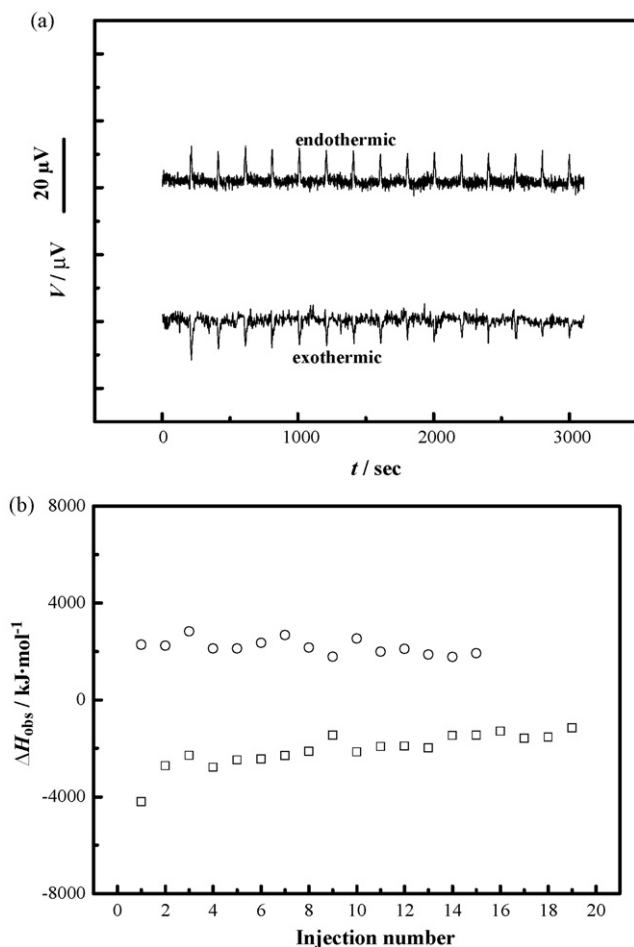
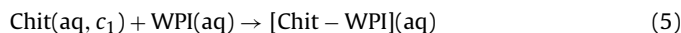


Fig. 2. Typical microcalorimetric titration curves for chitosan/WPI interaction. (a) Exothermic peaks show results from the titration of a WPI 0.5% (w/w) solution with chitosan 0.7% (w/w) solution at pH 6, and endothermic peaks represent the dilution of the chitosan solution into the pH 6 acetate buffer. (b) Area of the obtained peaks as a function of injection number. (□) Chitosan/WPI and (○) chitosan/acetate buffer.

can be written as



where reaction (4) represents the dilution of Chit into acetate buffer, giving the enthalpy of dilution of concentrated Chit DD solution to the final concentration in the vessel ($\Delta H_{\text{obs}}(4)$), and reaction (5) corresponds to the total process—dilution of Chit DD into WPI solution accompanied by the formation of Chit–WPI complex ($\Delta H_{\text{obs}}(5)$). Thus, the interaction enthalpies (ΔH_{int}) of chitosan with WPI can be calculated from the differences in observed enthalpy values with and without chitosan as,

$$\Delta H_{\text{int}} = \Delta H_{\text{obs}}(5) - \Delta H_{\text{obs}}(4) \quad (6)$$

ΔH_{int} therefore reflects a balance of various contributions: polymer dehydration, binding, electrostatic and hydrophobic interaction. The separation of these effects cannot be performed, as the thermodynamic property measured reflects the all process. The enthalpies of interaction between WPI and the two chitosan samples (with different DD) at the studied pH values (3–6), were calculated accordingly.

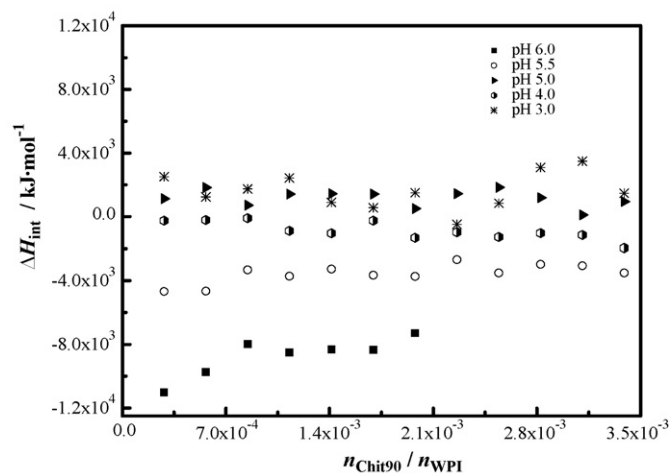


Fig. 3. Interaction enthalpies (ΔH_{int}) at 308.15 K for the titration of a 0.7% (w/w) Chit 90 solution into a 0.5% (w/w) WPI solution in acetate buffer 0.100 mol L⁻¹ at different pH values.

3.4. The effects of pH and degree of deacetylation (DD) on chitosan–WPI interactions

The effect of pH on the interaction between Chit and WPI was studied in the range of pH 3–6. The results obtained were treated as described above (Section 3.3) and the interaction enthalpies were calculated according to Eq. (6).

Figs. 3 and 4 show the variation of the interaction enthalpies (ΔH_{int}) with the molar ratios of chitosan to WPI ($n_{\text{Chit}}/n_{\text{WPI}}$) for the studied systems—Chit 90/WPI and Chit 95/WPI, at different pH values. The charge number/polymer mole depends on the molar mass and DD [26]. In the present case, the polymer with higher DD (95%) has a lower molar mass (see Table 1). This implies that Chit 90 has a higher charge number/polymer mole as compared to Chit 95, as it contains a higher degree of ionisable groups.

For Chit 90, we observe that for pH 6 and 5.5 the interaction enthalpies are exothermic, being about constant for pH 5.5 and decreasing (in absolute value) for pH 6 until a ratio ($n_{\text{Chit}}/n_{\text{WPI}}$) of about 0.00084, remaining constant thereafter. According to the literature, the isoelectric point of the main component of WPI, β -LG, is 5.2 [27,28]. Considering that the normal pK_a value of primary amines is around 6.5 [10,11], then Chi90 and β -LG should be oppo-

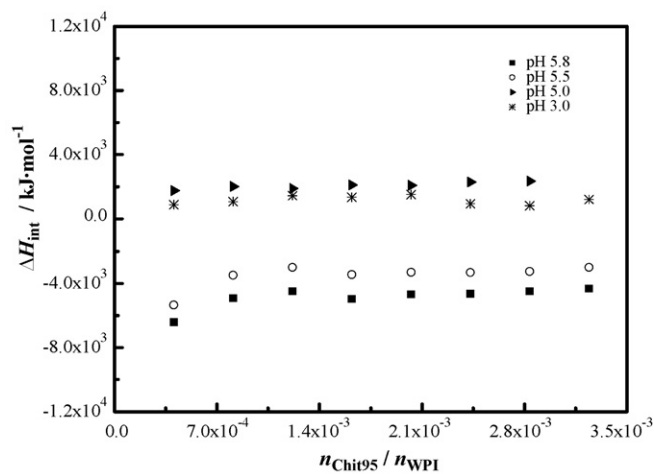


Fig. 4. Interaction enthalpies (ΔH_{int}) at 308.15 K for the titration of concentrated a 0.7% (w/w) Chit 95 solution into a 0.5% (w/w) WPI solution in acetate buffer 0.100 mol L⁻¹ at different pH values.

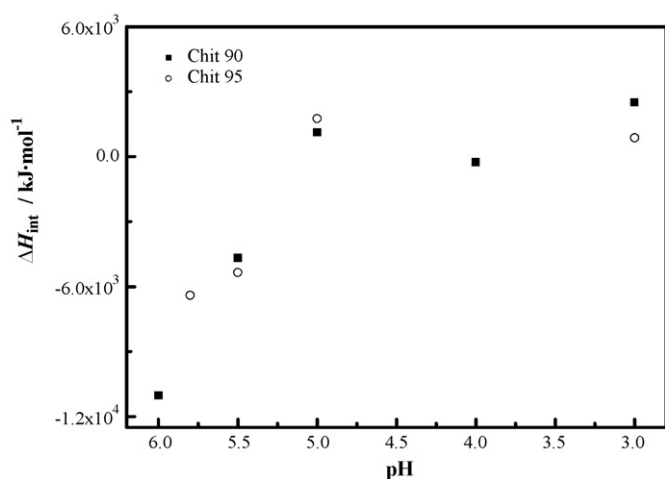


Fig. 5. Plot of the interaction enthalpy (ΔH_{int}) for the systems Chit DD–WPI, at the first injection, at different pH values. Chit 90 (■) and Chit 95 (○).

sitely charged at pH 6. Therefore, in the initial stage of the titration, the exothermic effect observed for the interaction can be ascribed to the electrostatic interaction between the positively charged chitosan and the negatively charged β -LG.

For $\text{pH} \leq 5$, the interaction enthalpy was zero (within uncertainty), showing that there is no significant interaction. At these pHs, β -LG is either neutral or slightly positively charged, and chitosan remains positively charged [29]. Therefore, probably the repulsion between polymer and protein plays a controlling role, overwhelming the other interaction, and producing a neat zero effect.

For Chit 95/WPI system the thermodynamic behaviour is similar to that of Chit 90/WPI systems (Fig. 4). The curves at pH 5.8 and 5.5 indicate again that an exothermic interaction takes place, which can be ascribed to the attractive electrostatic interactions between the oppositely charged WPI and chitosan. At pH 4 the interaction was very small and not significantly different from zero (data not shown).

As saturation is achieved at low Chit/WPI ratios for $\text{pH} \geq 5.5$ (Figs. 3 and 4), the most significant differences occur at first injections. In order to provide a general indication about the pH dependence of the WPI–chitosan interactions, the enthalpy changes associated with the first injection of chitosan solution (Chit 90 and Chit 95) have been plotted vs pH in Fig. 5. Clearly a critical value is found about pH 5, as the interaction enthalpies level off at this pH value. It should be stressed that this is close to the isoelectric point of the main component of the WPI mixture, i.e., β -LG.

Overall the trends obtained by ITC for both DDs did not show large differences, a reasonable result considering the small (5%) difference in deacetylation degree of the two chitosan samples—therefore the energetics are affected (absolute enthalpy values) but not the overall trend. Further, we can see that the levelling-off appears at similar Chit/WPI ratios ($n_{\text{Chit DD}}/n_{\text{WPI}}$), namely, between 0.00084 and 0.0011.

3.5. Turbidity

3.5.1. Effect of chitosan concentration on the interaction

As described in Section 2.3.4, UV–vis spectroscopy can be used to follow the change in optical dispersion (OD) that reflects the change in aggregation state in these mixtures. The increase in OD is associated with the formation of aggregates that remain suspended in the liquid matrix. The variation of OD with the Chit DD/WPI molar ratio ($n_{\text{Chit}}/n_{\text{WPI}}$) at different pH values is shown in Fig. 6 for Chit 90/WPI and in Fig. 7 for Chit 95/WPI. Again here the results are not signifi-

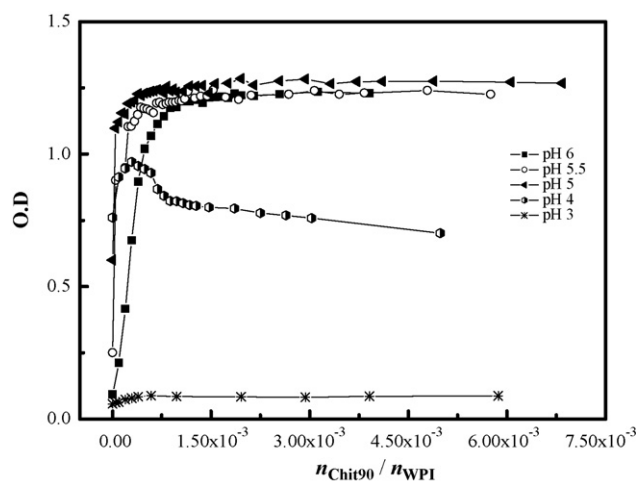


Fig. 6. Turbidity (optical dispersion) registered at different pHs for 900 μL of 0.5% (w/w) WPI solution in an acetate buffer 0.100 mol L^{-1} , and after the injection of 5 μL aliquots of a 0.14% (w/w) Chit 90 solution. The wavelength used was 400 nm and the temperature was kept constant at 308.15 K.

cantly different for Chit 90 and Chit 95, as also observed by ITC. For all studied pHs (except for pH 3) we observed a dramatic increase in the OD on the first chitosan additions ($0 < n_{\text{Chit90}}/n_{\text{WPI}} < 0.001$). This increase can be ascribed to the formation of a Chit–WPI complex (coacervate). At pH values around 6, the protein solution presents as expected a low turbidity (~ 0.08), due to the small mean diameter of the proteins in the WPI solution at these pH values. It is well known that β -LG exists as either monomers or dimers under these conditions [30].

After the initial raise in OD, for $\text{pH} > 5$ the values remain relatively constant after ($n_{\text{Chit90}}/n_{\text{WPI}} > 0.0013$, or 0.008 g dL^{-1}), suggesting that no more insoluble WPI–chitosan aggregates are formed as we increase Chit DD concentration, and that the ones formed remain stable. This is in very good agreement with the critical molar ratio ($n_{\text{Chit90}}/n_{\text{WPI}} = 0.001$) we found by ITC (Figs. 3 and 4). These results are also in good agreement with those previously reported by Guzey and McClements in the study of β -LG–chitosan interactions in aqueous solution [29], where they suggest the formation of an insoluble complex for chitosan concentrations higher than 0.01 g dL^{-1} .

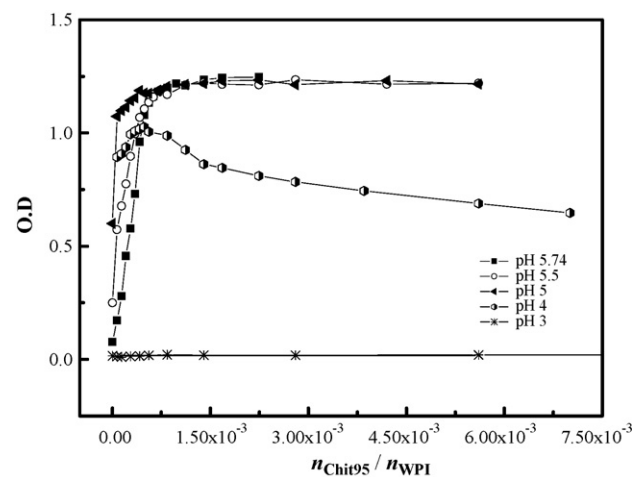


Fig. 7. Turbidity (optical dispersion) registered at different pHs for 900 μL of 0.5% (w/w) WPI solution in an acetate buffer 0.100 mol L^{-1} , and after the injection of 5 μL aliquots of a 0.14% (w/w) Chit 95 solution. The wavelength used was 400 nm and the temperature was kept constant at 308.15 K.

At pH 5, a much higher value was obtained for the optical dispersion in pure WPI solution. This can be explained by considering that a significant aggregation of β -LG takes place at this pH as we are very close to its isoelectric point ($pI=5.2$), and thus the protein is non-charged. In fact, it can be observed both in Figs. 6 and 7 that the initial OD value for pure WPI solution increases as the pH decreases.

Interestingly, the only different pattern for the Chit DD/WPI system is observed at pH 4 with both Chit 90 and Chit 95, as at this pH, after an initial increase in OD for very small chitosan concentrations (until a molar fraction of $n_{\text{chit90}}/n_{\text{WPI}} \approx 0.0005$), the values decrease smoothly but constantly. At pH 4 the charge of the main component, β -LG, should be positive, but it should be noted that the isoelectric point for α -LA (the minor component, 18%) is between 4.2 and 4.5. As a consequence, repulsive interactions are to be expected between chitosan and the major component after polymer addition to the system. But we also have to consider the presence of other interactions in Chi DD/WPI mixed systems at this pH—hydrogen bonding and hydrophobic interactions. In the low Chit DD concentration range, the increase in turbidity with increasing ratio ($n_{\text{chit90}}/n_{\text{WPI}}$) indicates the formation of Chi/WPI aggregates, even though that charges are the same—the main drive force here results from favourable hydrogen bonding and hydrophobic interaction. When $n_{\text{chit90}}/n_{\text{WPI}} > 0.0005$, the repulsive part controls the behaviour—after an initial increase, the turbidity decreases sharply for chitosan concentrations in the range of $0.001 > n_{\text{chit90}}/n_{\text{WPI}} > 0.0005$; for even higher ratios the turbidity decreased more slowly, in an almost linear way—this suggests that the continuing addition of chitosan is changing the aggregation state of the system, probably due to the repulsive interactions established between the similarly charged protein and chitosan. It seems as though the increase in chitosan concentration is inducing the formation of progressively smaller aggregates. In fact, the optical dispersion went down to values even lower than the initial one obtained for the protein alone, strongly suggesting that the charged chitosan is being able to dissolve or separate the fraction of protein that was uncharged and aggregated prior to chitosan addition.

We should note that by ITC we could not detect a significant interaction at pH 4, but we see a change in OD upon addition of chitosan at this pH. This shows that in terms of aggregation the systems are changing, but our instrument was not sensitive enough to detect the corresponding energy changes.

Finally the results obtained at pH 3 confirm all the hypotheses previously suggested. The initial turbidity was close to 0 (even lower than the obtained at pH 6) indicating the absence of a significant amount of insoluble and/or aggregated particles in solution. This fact must be explained by the high degree of charge in β -LG (as well as all other proteins in the mixture) at this pH value which prevents aggregation. The addition of chitosan had in this case a very small effect on optical dispersion. These results are in very good agreement with the results obtained by ITC.

3.5.2. The effect of pH on the turbidity of chitosan–WPI solutions

The addition of glacial acetic acid to a mixture of WPI and chitosan allows the study of the influence of pH on the aggregation of this system in the pH range between 6 and 3. For this, the turbidity of the mixture was monitored by spectrophotometry during acidification.

Figs. 8 and 9 present the results obtained for the mixtures containing Chit 90 and 95, respectively. The curves obtained for a pure WPI solution and for pure chitosan at two different concentrations (in acetate buffer) are included in both figures for comparison purposes. For WPI (open circles), the turbidity changes significantly with pH decrease—initially we observe a raise in OD as the pH decreases, going through a maximum at about 4.25 and decreasing thereafter steeply, reaching at pH 3 an OD value sim-

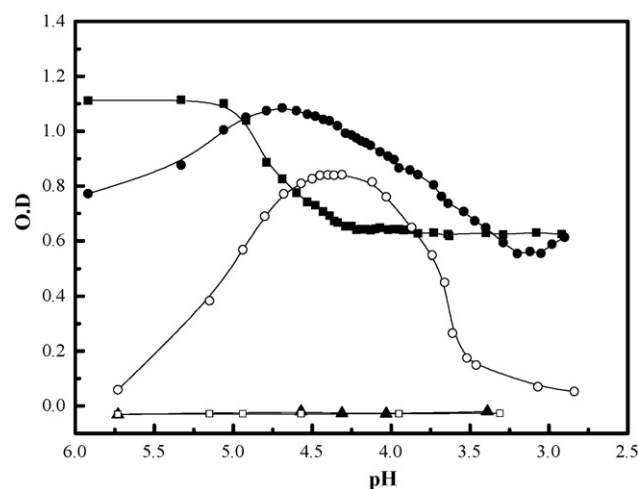


Fig. 8. Turbidity (optical dispersion) vs pH plots for a pure WPI solution (0.5% (w/w)), two pure Chit 90 solutions (2.37×10^{-3} and 2.40×10^{-2} g dL $^{-1}$), and their mixture. The wavelength used was 400 nm and the temperature was kept constant at 308.15 K. All solutions were prepared in acetate buffer 0.100 mol L $^{-1}$. (—●—) Mixture of Chit 90 (2.37×10^{-3} g dL $^{-1}$) and WPI (0.5% (w/w)); (—■—) mixture of Chit 90 (2.40×10^{-2} g dL $^{-1}$) and WPI (0.5% (w/w)); (—○—) WPI (0.5% (w/w)); (—▲—) Chit 90 (2.40×10^{-2} g dL $^{-1}$) and (—□—) Chit 90 (2.37×10^{-3} g dL $^{-1}$).

ilar to the one observed in the beginning (pH ~ 5.7). At pH < 3.5 and pH > 5.5 , where the main proteins in WPI are expected to have a high positive and negative charge, respectively, the turbidity is almost zero—the strong intermolecular repulsive electrostatic interactions at pH < 3.5 separates the protein molecules and the solution is pretty clear. At pH values intermediate to these ones, the change in protonation state of the WPI proteins makes them prone to association/aggregation. This observation is in good agreement with what was previously observed and discussed in Section 3.5.1.

The curves obtained for Chit 90 and Chit 95 at two different concentrations (see Section 2) are also shown in Figs. 8 and 9. The concentrations used correspond to two Chit/WPI ratios used in ITC: (a) equal to the one found after first injection and (b) equal to a ratio already in the plateau region (see Figs. 3 and 4). The polymer showed a negligible optical dispersion in the whole studied pH region, indicating that neither polymer does undergo aggre-

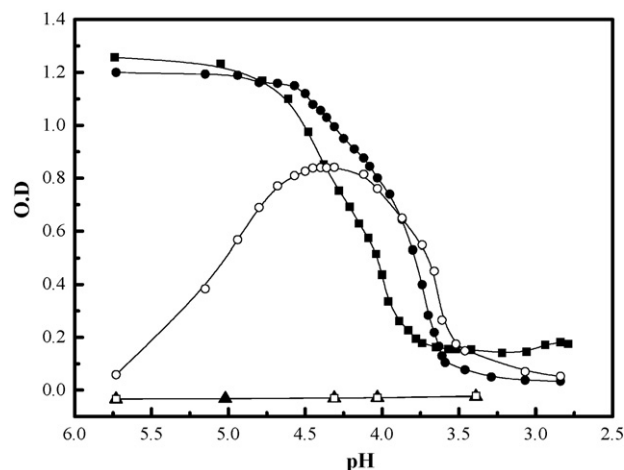


Fig. 9. Turbidity (optical dispersion) vs pH plots for a pure WPI solution (0.5% (w/w)), two pure Chit 95 solutions (2.37×10^{-3} and 2.40×10^{-2} g dL $^{-1}$), and their mixture. The wavelength used was 400 nm and the temperature was kept constant at 308.15 K. All solutions were prepared in acetate buffer 0.100 mol L $^{-1}$. (—●—) Mixture of Chit 95 (2.37×10^{-3} g dL $^{-1}$) and WPI (0.5% (w/w)); (—■—) mixture of Chit 95 (2.40×10^{-2} g dL $^{-1}$) and WPI (0.5% (w/w)); (—○—) WPI (0.5% (w/w)); (—▲—) Chit 95 (2.40×10^{-2} g dL $^{-1}$) and (—□—) Chit 95 (2.37×10^{-3} g dL $^{-1}$).

gate formation within this pH window. The curves obtained for the mixtures containing the WPI and Chit 90 for two Chit 90 concentration and same WPI concentration are shown in Fig. 8. The results obtained for the mixture richer in Chit 90 ($2.40 \times 10^{-2} \text{ g dL}^{-1}$) agree with the previously observed ones by ITC and turbidity (Section 3.5.1)—(a) a high optical dispersion was registered at pH 6, for which a strong chitosan–WPI attractive electrostatic interactions and the formation of insoluble coacervates is expected, (b) the OD starts to decrease at a pH value close to the isoelectric point of the main protein constituent of WPI (pH > 5) and remains constant for pH < 4.25. The curve shape is similar to a pH titration curve, meaning that we are observing the effect of protonation of the NH_2 groups in chitosan and the charged residues at the protein surface. Moreover, as no effect is observed for the polymer alone, this means that the protonation of the amino groups in the WPI/Chit complex builds up a charge that induces chain separation, and therefore the OD decreases. The solubilisation of the coacervates should be ascribed to the shift in the protein charge at pH < 5. The same experiment was performed at a lower chitosan concentration, $2.37 \times 10^{-3} \text{ g dL}^{-1}$. The curve has a shape similar to the one obtained for WPI except that the optical dispersion is higher in the whole pH window here studied. This can be explained as a result of the small amount of complex that could be formed at all pH values. Therefore, the shape of the titration curve reflects more the change in WPI protonation, superimposed by presence of complexes (higher OD), but less significantly influenced by the titration of the NH_2 groups in Chit 90 (the clear inflection point of the Chit 90 curve disappears in this case).

The same kind of experiment was performed using Chit 95. The results in Fig. 9 revealed this time a clear difference between the two chitosan sample systems with different DD and M_w . For the mixture containing Chit 95 at low concentration the results showed a significant difference as compared to the behaviour shown by Chit 90 for the same concentration. In fact, the shape of the curve is close to the one corresponding to the mixture richer in chitosan and very different from to the one for the pure WPI. It can be concluded from this results that when the DD is 95 at pH 6 significant amounts of coacervates were formed for both chitosan concentrations (Fig. 9, initial part of the titration curve, until pH values around 4.5), that react quite similarly to pH change, and therefore the increase in polymer concentration is not reflected in a different OD pattern. As stressed above, in our case the charge number/polymer mole is higher in Chit 90 than in Chit 95, due to the different molar masses of the two polymers. As such, one could expect a larger amount of complex formed in the case of Chit 90 at high pH. The fact that we observe the opposite, leads us to conclude that in this case a larger amount of insoluble complex is formed with Chit 95 because the difference in molar mass overwhelms the small difference in DD, as far as the complex formation is concerned.

Another important difference between Chit 90 and Chit 95 is the residual opacity of the mixtures at pH 3—we observe in Fig. 8 that OD is still around 0.5 at pH 3 (for both high and low Chit 90 concentrations). This suggests that the complexes formed with Chit 90 resist dissociation at low pH, contrary to the ones formed with Chit

95. For this sample with higher molar mass, the energy of interaction between chains will increase and therefore dissolution is reduced.

As a final conclusion, we would say that the results from ITC and turbidity measurements are complementary and provide very valuable insights into the nature of WPI–chitosan interactions and their dependence on changes in environment variables, such as concentration (WPI/Chit ratio), pH, molar mass and DD.

Acknowledgments

Thanks are also due to FCT for financial support to REQUIMTE and CIQ (UP) and for Post-Doc grants to H.K.S.S (SFRH/BPD/37514/2007) and GB (SFRH/BPD/41407/2007).

References

- [1] D.H.G. Pelegrine, C.A. Gaparetto, *Lebensm.-Wiss. u.-Technol.* 38 (2005) 77–80.
- [2] C. Holt, D. McPhail, T. Nylander, J. Otte, R.H. Ipse, R. Bauer, L. Øgendal, K. Olieman, K.G. de Kruijff, J. Léonil, D. Mollé, G. Henry, J.L. Maubois, M.D. Pérez, P. Puyol, M. Calvo, S.M. Bury, G. Kontopidis, I. McNaie, L. Sawyer, L. Ragona, L. Zetta, H. Molinari, B. Klarenbeek, M.J. Jonkman, J. Moulin, D. Chatterton, *Int. J. Food Sci. Technol.* 34 (1999) 587–601.
- [3] F. Shahidi, J.K.V. Arachchi, Y.-J. Jeon, *Trends Food Sci. Technol.* 10 (1999) 37–51.
- [4] K.A. Janes, M.J.J. Alonso, *Appl. Polym. Sci.* 88 (2003) 2769–2776.
- [5] J. Cho, M.-C. Heuzey, A. Bégin, P.J. Carreau, *Carbohydr. Polym.* 63 (2006) 507–518.
- [6] M. Thonggam, D.J. McClements, *Food Hydrocolloids* 19 (2005) 813–819.
- [7] V. Speiciene, F. Guilmineau, U. Kulozik, D. Leskauskaite, *Food Chem.* 102 (2007) 1048–1054.
- [8] S.L. Turgeon, C. Schmitt, C. Sanchez, *Curr. Opin. Colloid Interface Sci.* 12 (2007) 166–178.
- [9] S. De, D. Robinson, *J. Control. Release* 89 (2003) 101–112.
- [10] A.-L. Kjøniksen, B. Nystrom, C. Iversen, T. Nakken, O. Palmgren, T. Tande, *Langmuir* 13 (1997) 4948–4952.
- [11] A. Montilla, E. Casal, F.J. Moreno, J. Belloque, A. Olano, N. Corzo, *Int. Dairy J.* 17 (2007) 459–464.
- [12] A. Ababou, J.E. Ladbury, *J. Mol. Recogn.* 20 (2007) 4–14.
- [13] T. Harnsilawat, R. Pongsawatmanit, D.J. McClements, *Food Hydrocolloids* 20 (2006) 577–585.
- [14] R. Dimova, R. Lipowsky, Y. Mastai, M. Antonietti, *Langmuir* 19 (2003) 6097–6103.
- [15] G. Bai, J.A.M. Catita, M. Nichifor, M. Bastos, *J. Phys. Chem. B* 111 (2007) 11453–11462.
- [16] H. Zakariassen, M. Sørli, *Thermochim. Acta* 464 (2007) 24–28.
- [17] M.R. Kassai, *Carbohydr. Polym.* 68 (2007) 477–488.
- [18] G. Bai, L.M.N.B.F. Santos, M. Nichifor, A. Lopes, M. Bastos, *J. Phys. Chem. B* 108 (2004) 405–413.
- [19] C. Matos, J.L.C. Lima, S. Reis, A. Lopes, M. Bastos, *Biophys. J.* 86 (2004) 946–954.
- [20] L.-E. Briggner, I. Wadsö, *J. Biochem. Biophys. Meth.* 22 (1991) 101–118.
- [21] M. Bastos, S. Hägg, P. Lönnbro, I. Wadsö, *J. Biochem. Biophys. Meth.* 23 (1991) 255–258.
- [22] P. Bäckman, M. Bastos, L.-E. Briggner, S. Hägg, D. Hallén, P. Lönnbro, S.-O. Nilsson, G. Olofsson, A. Schön, J. Suurkuusk, C. Teixeira, I. Wadsö, *Pure Appl. Chem.* 66 (1994) 375–382.
- [23] S.M. Fitzsimons, D.M. Mulvihill, E.R. Morris, *Food Hydrocolloids* 21 (2007) 638–644.
- [24] Z.Y. Ju, N. Hettiarachchy, A. Kilara, *J. Dairy Sci.* 82 (1999) 1882–1889.
- [25] C.-Y. Ma, V.R. Harwalkar, *Adv. Food Nutr. Res.* 35 (1991) 317–366.
- [26] S.M. Taghizadeh, G. Davari, *Carbohydr. Polym.* 64 (2006) 9–15.
- [27] M. Verheul, J.S. Pedersen, S.P.F.M. Roefs, K.G. Kruijff, *Biopolymers* 49 (1999) 11–20.
- [28] J.S. Mounsey, B.T. O’Kennedy, M.A. Fenelon, A. Brodtkorb, *Food Hydrocolloids* 22 (2008) 65–73.
- [29] D. Guzey, D.J. McClements, *Food Hydrocolloids* 20 (2006) 124–131.
- [30] P.R. Majhi, R.R. Ganta, R.P. Vanam, E. Seyrek, K. Giger, P.L. Dubin, *Langmuir* 22 (2006) 9150–9159.